Influence of Surface Roughness Factor in Modeling Isothermal Piston Skirts Lubrication in Initial Engine Start Up

S. Adnan Qasim, Mubashir Gulzar, M. Afzaal Malik.

Abstract— **Initial engine start-up is an occasion when wear of the interacting piston skirts and the liner surfaces cannot be avoided. Adhesive wear is more pronounced in a few initial cycles of the cold engine start-up. It occurs due to the absence of a fully established lubricant film between the skirt and the liner surfaces. The skirt and the liner surfaces are essentially rough with different asperity amplitudes. The different deterministic asperity amplitudes are anticipated to influence the formation of hydrodynamic lubricating film at low start-up loads significantly. This study numerically models the hydrodynamic lubrication of piston skirts by defining the secondary piston motion and the geometry of the interacting skirts and the liner surfaces as functions of 720 degree crank rotation cycle. The 2-D Reynolds equation is solved numerically after incorporating the different asperity amplitudes to study their influence on the generated hydrodynamic pressures, lubricant film thickness, and secondary piston displacements. A high viscosity-grade engine lubricant, low load and engine start-up speed under isothermal conditions are some of the salient characteristics of the 2-D model. The simulation results show that the different roughness asperity amplitudes improve the hydrodynamic film thickness and affect the piston secondary displacements, surface energy transfer, hydrodynamic pressures and load-carrying capacity of the film in a few engine start-up cycles.**

Index Terms— **Initial Engine Start-up, Roughness, Asperity Amplitude, Hydrodynamic Lubrication, Piston Skirt.**

I. Introduction

The moving components of an internal combustion (IC) engine are exposed to the contact friction and adhesive wear of their interacting surfaces at the time of the initial engine start up. The rough surfaces of the piston skirts and the cylinder liner are vulnerable to a physical contact in the absence of a sufficiently thick fully developed lubricant film and the secondary translations of the piston. The secondary piston motion generates slap and noise due to the extra radial clearance between the skirts and the liner surfaces. The cumulative effects of the secondary transverse piston motion, starvation, cavitation and the rough asperities of the surfaces alter the contact geometry and the lubricant film thickness. In this context the amplitudes of the asperities play an important role towards the effective film thickness profile. Hamilton et al developed a theory of hydrodynamic lubrication between the two parallel surfaces with the surface roughness on one or both of the surfaces. It does not predict the existence of any pressure in case of the sliding flat parallel surfaces [1]. Surface roughness helps in the buildup of pressures between the two interacting surfaces. Tzeng and Saibel concluded that the load carrying capacity and the frictional forces increase considerably when the surface roughness is taken into account [2]. When the mean separation of the sliding surfaces is small as compared to the roughness amplitudes, the roughness effects become significant. It happens when the surfaces come close to each other [3]. Patir and Cheng presented a model based on the flow factors which were introduced to modify the average Reynolds equation [4]. In that model the functional dependence of the factors on the roughness parameters can only be inferred from the numerical experiments and expressed in the fitted form. Tripp et al presented their work in which the problems associated with the Patir and Cheng model were addressed [5]. Greenwood et al investigated the effects of transverse surface roughness in the elastohydrodynamic lubrication [6]. From all these cases it is evident that the rough surface amplitudes play a significant role in influencing the film thickness profiles and the load-carrying capacity of the lubricant. To model the lubrication of the piston skirts in the initial engine start-up and study the influence of the roughness factor, the logical assumptions are :

1. Newtonian lubricant with thermal effects neglected
2. Pressure at the inlet of contact zone is zero.
3. Flow is laminar and turbulence effects are neglected.
4. Surfaces are oil-flooded at the time of engine start up.

II. Mathematical Model

A. Equations of Piston Motion

The position of the piston, its velocity and acceleration along the axis of the cylinder are dependent on the crank angle. For constant crankshaft speed, piston speed is [7]:

$$U = \dot{Y} r\omega \sin\psi + r\omega B \cos\psi (l^2 - B^2)^{-0.5} \quad (1)$$

where $B = C_p r \sin\psi$ (2)

This work was sponsored by National University of Sciences and Technology (NUST), Islamabad, Pakistan. Financial support was provided by the Higher Education Commission of Pakistan.
Syed Adnan Qasim is Research Associate at NUST College of Electrical and Mechanical Engineering, Rawalpindi (email: adnan_qasim@yahoo.com)
Mubashir Gulzar is Lecturer at NUST College of Electrical and Mechanical Engineering, Rawalpindi (email: mubashir_nustian@hotmail.com)
M. Afzaal Malik is Professor at Department of Mechanical and Aerospace Engg, Air University, Islamabad (email: drafzaalmalik@yahoo.com)

ISBN: 978-988-19252-2-0
ISSN: 2078-0958 (Print); ISSN: 2078-0966 (Online)

Table-1 (Input Parameters)

Parameter	Value	Parameter	Value
m_{pis}	0.295 kg	$\Theta = \theta_1 + \theta_2$	75 degree
R	0.0415 m	l	0.133 m
L	0.0338 m	η	0.0857 Pa.s.
m_{pin}	0.09 kg	υ_1, υ_2	0.3
R	0.0418 m	E_1, E_2	200 GPa

During its axial translation the piston displaces eccentrically in the transverse direction. The equations, which are used to define the secondary piston motion along the direction perpendicular to the axis of the cylinder are duly incorporated in the mathematical model. To determine the secondary eccentricities of the piston skirts, the inertia of the piston, the sum of the forces and their moments are considered. To calculate the eccentricities of the top and the bottom surfaces of the skirts, the forces and the moments are used in the form of the force and moment balance equations similar to that defined by Zhu et al [7]:

$$\begin{bmatrix} a_{11} & a_{22} \\ a_{21} & a_{22} \end{bmatrix} \begin{bmatrix} \ddot{e}_t \\ \ddot{e}_b \end{bmatrix} = \begin{bmatrix} \mathrm{F} + \mathrm{F_s} + F_f \tan\phi \\ M + M_s + M_f \end{bmatrix} \tag{3}$$

$$a_{11} = m_{pin}\left(1 - \frac{a}{L}\right) + m_{pin}\left(1 - \frac{b}{L}\right) \tag{4}$$

$$a_{12} = m_{pin}\left(\frac{a}{L}\right) + m_{pin}\left(\frac{b}{L}\right) \tag{5}$$

$$a_{21} = \left(\frac{I_{pin}}{L}\right) + m_{pin}(a-b)\left(1 - \frac{b}{L}\right) \tag{6}$$

$$a_{22} = m_{pin}(a-b)\left(\frac{b}{L}\right) - \left(\frac{I_{pin}}{L}\right) \tag{7}$$

$$F_s = \tan\phi\left(F_G + \tilde{F}_{IP} + \tilde{F}_{IC}\right) \tag{8}$$

$$M_s = F_G C_p + \tilde{F}_{IC} C_g \tag{9}$$

B. Calculation of Hydrodynamic Pressures

The 2-D Reynolds equation is solved numerically to calculate the hydrodynamic pressures generated over the surface of the piston skirts. The Reynolds equation is [8]:

$$\frac{\partial}{\partial x}\left(\frac{h^3 \partial p}{\partial x}\right) + \frac{\partial}{\partial y}\left(\frac{h^3 \partial p}{\partial y}\right) = 6U\eta \frac{dh}{dx} \tag{10}$$

C. Boundary Conditions

Boundary conditions for the Reynolds equation are [8]:

$$\frac{\partial p}{\partial x_{\theta=0}} = \frac{\partial p}{\partial x_{\theta=\pi}} = 0$$

$$p = 0 \qquad \text{when } x_1 \le x \le x_2$$

$$p(\theta, 0) = p(\theta, L) = 0 \tag{11}$$

D. Calculation of Hydrodynamic Film Thickness

The magnitude of gas force F_G is a function of crank rotation angles for the 720 degree cycle. The lubricant film thickness is given by [7, 9]:

$$h = C + e_t(t)\cos x + \left[e_b(t) - e_t(t)\right]\frac{y}{L}\cos x \tag{12}$$

where, $\theta = x/R$

E. Calculation of Surface Roughness Factor

The factors representing the amplitudes of the rough surface asperities of the skirts and the liner are introduced, as defined by Mistry and Priest [10]. The total film thickness after considering the surface roughness factors is given by:

$$h_T = h - \frac{\sigma}{\sqrt{2\pi}} \tag{13}$$

where $\sigma = \sqrt{(\sigma_1{}^2 + \sigma_2{}^2)}$ (14)

where σ_1(μ m) = Surface roughness of Skirts = 1.515 [11]
σ_2(μ m) = Surface roughness of the Liner = 1.715 [11]

F. Non-Dimensionalization

In non-dimensional form the Reynolds equation is [8]:

$$\frac{\partial}{\partial x^*}\left(h^{*3}\frac{\partial p^*}{\partial x^*}\right) + \left(\frac{R}{L}\right)^2 \frac{\partial}{\partial y^*}\left(h^{*3}\frac{\partial p^*}{\partial y^*}\right) = \frac{\partial h^*}{\partial x^*} \tag{15}$$

G. Discretization

To solve the Reynolds equation numerically a finite difference mesh is geerated and an explicit numerical scheme is used to determine the hydrodynamic pressures at each node of a 21x21 nodes mesh. For better comprehension the Vogelpohl parameter M_v is introduced [8]. It has the following relationship with the hydrodynamic pressure [8]:

$$M_v = p^* h^{*1.5^-} \tag{16}$$

$$M_{v,i,j} = \frac{C_1\left(M_{v,i+1,j} + M_{v,i-l,j}\right) + \left(\frac{R}{L}\right)^2 C_2\left(M_{v,i,j+l} + M_{v,i,j-i}\right) - G_{i,j}}{2C_1 + 2C_2 + F_{i,j}} \tag{17}$$

where $C_1 = \dfrac{1}{\delta x^{*2}}$; $C_2 = \dfrac{1}{\delta y^{*2}}$

The eccentricities $e_t(t)$ and $e_b(t)$ are calculated by solving equation (3). It constitutes an initial value problem for the two non-linear second order differential equations [7]. The values of e_t, e_b, $\dot{e}_t$ and $\dot{e}_b$ are assumed at the previous time step. The assumed values are used as the initial values for the current time step. Based on these values the mean hydrodynamic film thickness is calculated by solving equation (6). When the values of the eccentric displacement rates $\dot{e}_t$, $\dot{e}_b$ are satisfied and achieved, the piston position at the end of the current time step is obtained as [11, 12]:

$$e_t(t_i + \Delta t) = e_t(t_i) + \Delta t \dot{e}_t(t_i)$$

$$e_b(t_i + \Delta t) = e_b(t_i) + \Delta t \dot{e}_b(t_i)$$

We compute and satisfy the secondary acceleration terms $\ddot{e}_t$, $\ddot{e}_b$. These are satisfied from the solution of velocities $\dot{e}_t$, $\dot{e}_b$ at the previous and present time steps. The simulation of second

ISBN: 978-988-19252-2-0
ISSN: 2078-0958 (Print); ISSN: 2078-0966 (Online)

order differential equations show rigid hydrodynamic lubrication of piston skirts at respective time steps or crank angles [12]. The Newtonian lubricant is used in the numerical scheme for the lubrication solution. The average Reynolds equation is solved to calculate the distribution of hydrodynamic pressures. The gradients of pressure depend on the film thicknesses. Gauss Seidel iterative numerical scheme is used to solve the Reynolds and the oil film thickness equations simultaneously. The simulation results of the lubrication models correspond to the 720 degree crank rotation and show maximum and minimum film thicknesses and pressure fields [12].

III. Numerical Results and Discussion

To study the influence of the surface roughness factor, the mathematical model is solved numerically and then simulated to generate the results for the analysis. The salient input parameters include 10 microns piston-to-bore radial clearance, a high-viscosity grade lubricant of dynamic viscosity 0.1891 Pa.s. and the initial engine start up speeds of 500 and 600 rpm, respectively. The 720 degree crank rotation cycle has the 0-180 degree induction stroke, 181-360 degree compression stroke, 361-540 degree expansion stroke and 541-720 degree exhaust stroke. The simulation results show the profiles of the secondary piston eccentricities, secondary velocities, the maximum and the minimum hydrodynamic film thicknesses, the friction coefficient and the hydrodynamic pressures generated over the surface of the skirts. The simulation results are plotted as functions of 720 degree crank rotation cycle.

A. Piston Eccentricities

Figure 1 shows the secondary eccentric displacements of the top and the bottom surface of the piston skirts at 500 and 600 rpm initial engine start up speeds. The E_t and the E_b curves represent the profiles of the dimensionless eccentricities of the top and the bottom sides of the piston skirts. Figures 1 and 6 show the three horizontal lines such that the upper line at +1 and the lower line at -1 represent the non-thrust and the thrust sides of the cylinder liner wall surfaces, respectively. The center-line at '0' represents the fully concentric position of the piston with the liner surface. If the E_t *or* the E_b curve touches either the upper line or the lower line during the piston travel in the 4-stroke 720 degree cycle, then there is a physical contact between the rough skirts and the liner surfaces. Such a contact will damage the surface asperities, cause the plastic flow of material and adhesive wear of the interacting surfaces. The piston speed during each stroke of its travel is cyclic in nature. In each stroke the piston attains the maximum speed at the mid-stroke and has a minimum speed at the respective top and the bottom dead centers. Figures 1 shows generally similar E_t and the E_b curve profiles, however there are significant noticeable differences. At both the start up speeds the piston displaces concentrically in the first half of the induction stroke. After attaining the maximum cyclic speed at the mid-induction stroke at very small film thickness, the piston starts decelerating and loses energy. The hydrodynamic film thickness starts increasing and the piston gets displaced eccentrically towards the non-thrust side. At the completion of the induction stroke the piston changes its direction of travel and commences journey towards the top dead center (TDC). It displaces the piston skirts further towards the non-thrust side of the liner. The piston accelerates, compresses the air-fuel charge and accelerates in the first half of the compression stroke. There is a continuous transfer of energy from the skirts to the liner surface and the film thickness increases. At the end of the compression stroke the magnitude of the gas pressure force increases considerably as the air-fuel mixture is confined to the clearance volume. Combustion occurs at 372 degree of the crank angle [7]. The tremendous thrust produced due to combustion displaces the skirts towards the center-line. Resultantly, there is an instantaneous concentricity of the piston and the liner. However, the skirt surfaces move past the center-line and come very close to the lower line. It happens due to the inertia of the piston as a result of the excessive energy transfer and the subsequent second-order changes in the secondary displacement rates. The thrust generated due to combustion subsides as the piston approaches the bottom dead center at the end of the expansion stroke. The exhaust valves open and the piston pushes the burnt gases out of the combustion chamber in the exhaust stroke. The very low hydrodynamic pressures, insignificant magnitude of the gas pressure force and the energy transfer from the liner to the skirt surfaces do not permit any further displacement of the skirt surfaces till the completion of the 4-stroke cycle. A comparison of the differences in the eccentricity profiles at 500 and 600 rpm speeds shows some clear improvements in the profiles. At 600 rpm speed there is a reduction in the magnitude of the maximum eccentricities in the compression and the expansion strokes. It implies that the given amplitudes of the asperities of the rough surfaces of the skirts and the liner facilitate towards avoiding a possible contact and wear as the very low start up speed is increased slightly. Such a finding is in sharp contrast to the case where the roughness effects are neglected in the hydrodynamic lubrication regime due to which the skirts establish a physical contact with the liner surface in the expansion stroke [12].

B. Piston Secondary Velocities

Figures 2 shows the dimensionless secondary velocities or the displacement rates at 500 and 600 rpm start up speeds. The secondary velocities of the top and the bottom surface of the skirts are represented by the E_{tdot} and E_{bdot} profile curves, respectively. The secondary velocities of the skirts vary with the eccentric displacements of these surfaces in the 720 degree cycle. The secondary velocities of the top and the bottom surfaces have similar profiles at both the speeds except for a few minor differences in the magnitudes. Such differences indicate the different amounts of energy transfer between the skirts and the liner surfaces at each very low start up speed. The velocity profiles are plotted in the positive and the negative quadrants. The displacement rates in the positive quadrants imply the energy transfer from the skirts to the liner surface whereas the velocity profiles in the negative quadrant show the energy transfer from the liner to the skirts. The secondary velocities attain the maximum values in the expansion stroke as the maximum amount of energy is transferred after combustion. At 500 rpm slightly more energy is transferred after combustion than at 600 rpm speed. This extra energy is utilized in bringing the top surface of the skirts slightly closer to the thrust side of the liner, as shown in figure 1. The maximum transfer of energy from the from the liner to the skirts is almost the same, resulting in the similar eccentricity profiles in the exhaust stroke.

ISBN: 978-988-19252-2-0
ISSN: 2078-0958 (Print); ISSN: 2078-0966 (Online)

C. Hydrodynamic Film Thickness

Figure 3 shows the maximum and the minimum film thickness profiles as the function of 720 degree crank cycle. The maximum film thickness (denoted by max. hyd. film) is the condition prior to the application of the load, squeeze out effect and side leakages. The minimum film thickness carries the hydrodynamic loads and is denoted by *min. hyd. film*. The profiles show that the film thickness increases with the piston eccentricities in the induction and the compression strokes. The peak values are obtained prior to combustion. A sudden reduction in the thickness occurs in the expansion stroke but it increases again in the exhaust stroke. Except for a few minor variations the film thickness does not change with the change in the low engine start up speed.

D. Coefficient of Friction

Figure 4 shows the friction coefficient profiles as the function of 720 degree crank rotation cycle. A comparison of the profiles of friction coefficient at 500 and 600 rpm speeds shows that the energy loss increases quite significantly in the induction stroke. The energy loss is contained slightly during the second half of the expansion and during the exhaust strokes. It implies that the induction and the compression strokes of the piston contribute towards the maximum loss of energy and power at the very low engine start up speeds.

E. Hydrodynamic Pressures

The hydrodynamic pressures are generated due to the Poiseulle flow and the wedging action between the piston skirts and the liner surfaces. The 3-D dimensionless pressure fields are generated over the rough surface of the skirts at each degree of the 720 degrees crank rotation cycle. However, the space limitations permit simulation results of 3-D fields at some of the critical piston positions. Figures 5 and 6 show the pressure fields at the mid and the end-strokes of the piston at 500 and 600 rpm, respectively. A comparison of the pressures in the induction stroke shows the buildup of the low intensity positive pressures over the bottom surface of the skirts. In the compression stroke the gentle slopes are transformed into the steep gradients with sharply rising pressures over the surface of the bottom half of the skirts. The influence of the rough surface asperities causes the hydrodynamic pressures to build up over the bottom half with peak pressures rising over the bottom surface of the skirts. From figure 1 it is obvious that the smaller amplitudes of the eccentricities of the bottom surface rule out the possibility of a physical contact between the skirts and the liner. Such a buildup of pressures is in sharp contrast to the similar buildup over the top surface of the skirts when the influence of the surface roughness is neglected [12]. At 500 rpm speed the bias of the positive pressures remain towards the bottom surface in the first half of the expansion stroke. At 600 rpm the bias shifts over to the top surface of the skirts. It implies that the top surface carries the tremendous load after combustion and its close proximity with the liner surface increases the chances of a possible contact and wear. In the second half of the expansion stroke and the first half of the exhaust stroke the intensities of the pressures subside but they remain biased towards the top surface at both the speeds.

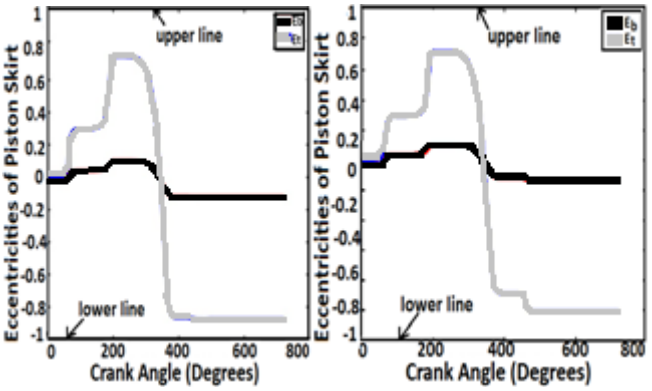

(a) (b)

Figure 1. Dimensionless piston eccentricities at (a) 500 rpm (b) 600 rpm

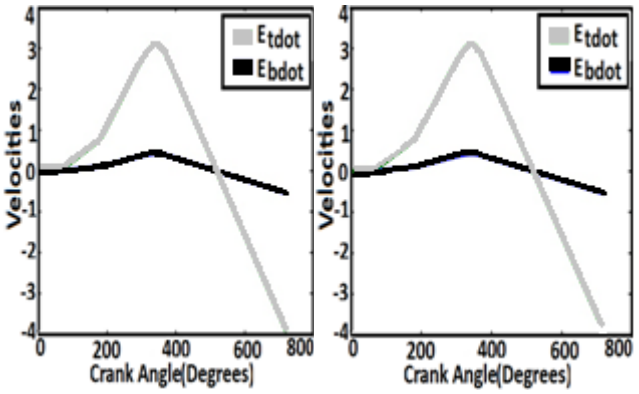

(a) (b)

Figure 2. Dimensionless secondary velocities at (a) 500 rpm (b) 600 rpm

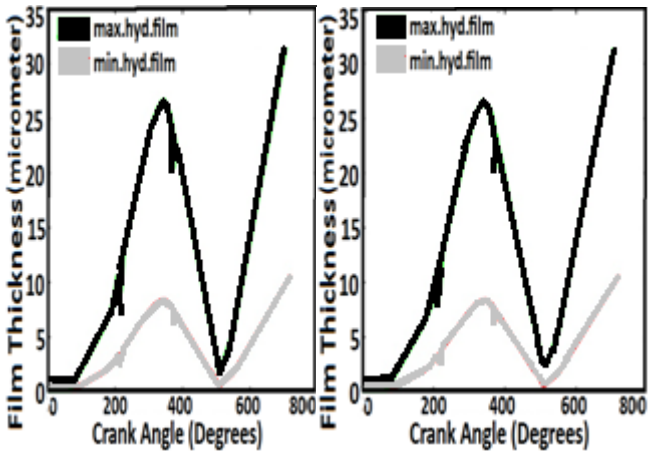

(a) (b)

Figure 3. Hydrodynamic film thickness at (a) 500 rpm (b) 600 rpm

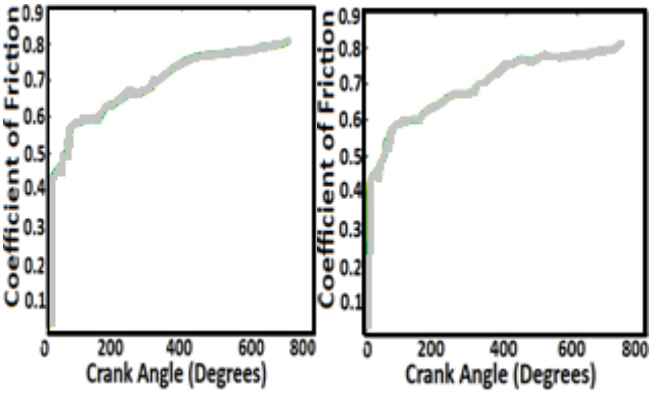

(a) (b)

Figure 4. Coefficient of friction Vs crank angle at (a) 500 rpm (b) 600 rpm

ISBN: 978-988-19252-2-0
ISSN: 2078-0958 (Print); ISSN: 2078-0966 (Online)

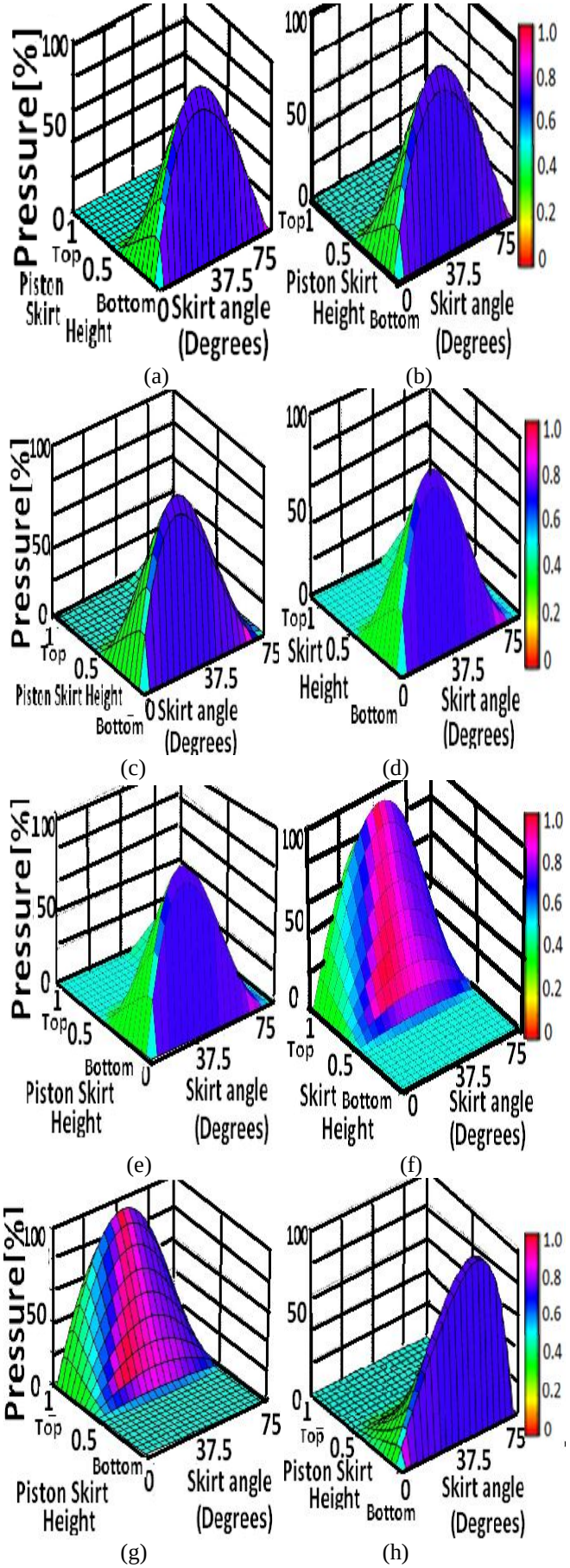

Figure 5. Dimensionless 3-D hydrodynamic pressure fields at 500 rpm at degree (a) 90 degree (b) 180 degree (c) 270 degree (d) 360 degree (e) 450 degree (f) 540 degree (g) 630 degree (h) 720 degree

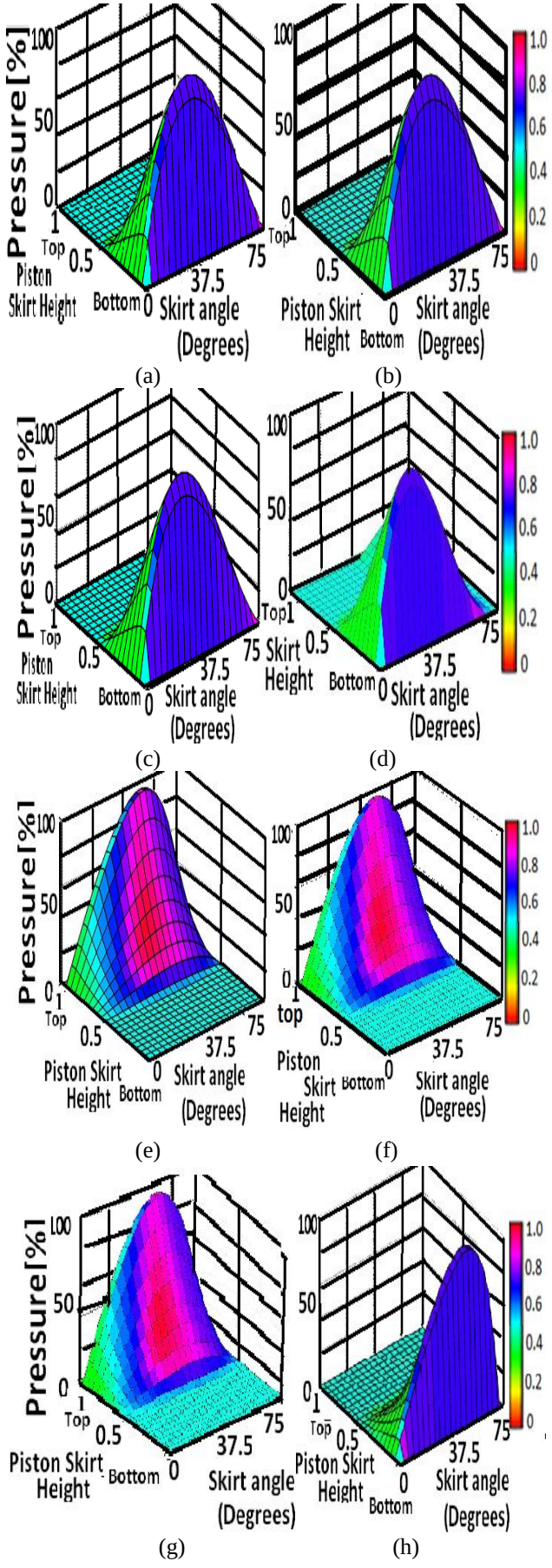

Figure 6. Dimensionless 3-D hydrodynamic pressure fields at 600 rpm at degree (a) 90 degree (b) 180 degree (c) 270 degree (d) 360 degree (e) 450 degree (f) 540 degree (g) 630 degree (h) 720 degree

ISBN: 978-988-19252-2-0
ISSN: 2078-0958 (Print); ISSN: 2078-0966 (Online)

IV. Conclusions

The work numerically models the piston skirts lubrication at the two very low initial engine start up speeds. The aim is to study the degree of influence exerted by the surface roughness factor on the critical hydrodynamic lubrication characteristics. At 500 rpm speed, a possible contact between the skirts and the liner surfaces may be avoided in the compression and the expansion strokes under the influence of the surface roughness factor. At 600 rpm speed the secondary piston eccentricities decrease further to minimize the chances of adhesive wear. Neglecting the influence of the roughness factor may invite a possible contact and wear of the surfaces. The amount of energy transfer and the power loss due to friction differ slightly at the two stated speeds. The buildup of the hydrodynamic pressures shows that there are more chances of a physical contact under the lubrication starvation conditions during the first half of the expansion stroke, when the start up speed is 600 rpm. With the lubrication flooding the eccentricities decrease at 600 rpm speed. Hence, 600 rpm speed may be recommended under the oil flooding conditions and 500 rpm is recommended when the partial or mixed lubrication conditions exist. Before reaching to a definite conclusion further studies are recommended at the other low engine start up speeds and under the variable load conditions.

Nomenclature

C = Piston radial clearance
C_f = Specific heat of lubricant
C_g = Distance from piston center of mass to piston pin
C_p = Distance of piston-pin from axis of piston
E_1, E_2 = Young's Modulus of piston and liner
F = Normal force acting on piston skirts
F_f = Friction force acting on skirts surface
F_{fh} = Friction force due to hydrodynamic lubricant film
F_G = Combustion gas force acting on the top of piston
F_h = Normal force due to hydrodynamic pressure in the film
F_{IC} = Transverse Inertia force due to piston mass
$\widetilde{F_{IC}}$ = Reciprocating Inertia force due to piston mass
F_{IP} =Transverse Inertia force due to piston-pin mass
$\widetilde{F_{IP}}$ = Reciprocating Inertia force due to piston-pin mass
I_{pis} = Piston rotary inertia about its center of mass
L = Piston skirt length
M = Moment about piston-pin due to normal forces
M_f = Moment about piston-pin due to friction force
M_{fh} = Moment about piston pin due to hydrodynamic friction
M_h = Moment about piston pin due to hydrodynamic pressure
R = radius of piston
U = Piston Velocity
a = Vertical distance from piston skirt top to piston pin
b = Vertical distance from piston skirt top to center of gravity
$\ddot{e}_b$ = Acceleration term of piston skirts bottom eccentricities
$\ddot{e}_t$ = Acceleration term of piston skirts top eccentricities
l = Connecting rod length
m_{pis} = Mass of piston
m_{pin} = Mass of piston pin
p = Hydrodynamic pressure
r = Crank radius
$\acute{r}$ = Radius of piston
u = Lubricant velocity component along x direction
v = Lubricant velocity component along y direction
τ = Shear stress
ψ = Crank angle
η = Viscosity at ambient conditions
Φ = Connecting rod angle
ω = Crank rotation speed
υ_1, υ_2 = Poisson's ratio
υ = Elastic deformation of piston skirts
θ = Piston skirts angle in degree

REFERENCES

[1] D. B. Hamilton, J. A. Walowit and C. M. Allen, "A theory of lubrication by micro-irregularities.", J. Basic Eng. Trans. ASME, Ser. D., pp. 177-185, March 1966.

[2] S. T. Tzeng, and E. Saibel, "Surface roughness effects on slider bearing lubrication." ASLE Trans. vol. 10, , pp 334-338, 1967.

[3] H. Christensen, "Stochastic models for hydrodynamic lubrication of rough surfaces." Proc. I. Mech.E, Tribol. Group 184, part 1, vol. 55, pp. 10-13. 1969-70.

[4] N. Patir, and H. S. Cheng, "An average flow model for determining the effects of three-Dimensional roughness on partial hydrodynamic lubrication, ASME J. lubrication technology, vol. 100(1), pp. 12-17, 1978.

[5] J. H. Tripp, "Surface roughness effects in hydro- dynamic lubrication: the flow factor method", ASME J. Lubrication Technology, vol. 105, pp. 458-463, 1983.

[6] A. Greenwood, & J. H. Tripp, "The Contact of Two Nominally Flat Rough Surface", Proc. Institution of Mechanical Engineers (IMechE), UK, (185), 1971, 625-633.

[7] D. Zhu, H. S. Cheng, T. Arai, and K. Hamai, "A numerical analysis for piston skirts in mixed lubrication", ASME J. Tribol., vol. 114(3), pp. 553-562, 1992.

[8] G. W. Stachowiak and A. W. Batchelor, Engineering Tribology, 3rd ed., Elsevier, USA, 2005, pp. 91-325.

[9] S. Adnan Qasim, M. A. Malik, M. A. Khan, and R. A. Mufti, "Low viscosity shear heating in piston skirts EHL in the low initial engine start up speeds", Tribol. International, vol. 44(10), pp. 1134-1143, September 2011

[10] K. N. Mistry, M. Priest, "Prediction of the lubrication regimes and friction of piston ring assembly of an I.C. engine considering the effect of surface roughness", Proc. 33rd Leeds –Lyon Symposium on Tribol. September12 -15, 2006.

[11] J. Yang, W. Yang, X. Yu, and C. Wang, "Design of internal combustion engine piston based on skirt lubrication analysis", SAE Technical Paper Series, 2001-01-2486.

[12] S. Adnan Qasim, M. Afzaal. Malik, U. F. Chaudhri, January 2012, "Analyzing Viscoelastic Effects in Piston Skirts EHL at Small Radial Clearances in Initial Engine Start Up", Tribology International, Vol. 45, Issue 1, pp. 16-29.

ISBN: 978-988-19252-2-0
ISSN: 2078-0958 (Print); ISSN: 2078-0966 (Online)